УДК 539.14 539.16

ON THE MASS SURFACE AND THE PROPERTIES OF NUCLIDES CLOSE TO HYPOTHETIC DOUBLY MAGIC LEAD-164

***V.I.Isakov*[1], *K.I.Erokhina*[2], *B.Fogelberg*[3], *Yu.N.Novikov*[1], *H.Mach*[3], *K.A.Mezilev*[1]**

The work presents calculations of the mass values and the decay energies for a set of nuclei close to the extreemely remote from the stability line ^{164}Pb. Different decay modes of the mentioned nuclide, as well as the properties of excited states of isobars with $A = 164$ and close to ^{164}Pb, are carefully examined.

The investigation has been performed at the St.Petersburg Nuclear Physics Institute, RAS, Physicotechnical Institute, RAS, and Department of Radiation Sciences, Uppsala University.

О массовой поверхности и свойствах ядер вблизи гипотетического дважды магического нуклида свинца-164

В.И.Исаков и др.

Проведены расчеты массовой поверхности и энергий распада для совокупности ядер вблизи предельно удаленного от дорожки стабильности нуклида ^{164}Pb. Изучены различные моды распада этого ядра, а также свойства возбужденных состояний ряда изобар с $A = 164$, близких к ^{164}Pb.

Работа выполнена в Петербургском институте ядерной физики РАН, Физико-техническом институте РАН и Отделе радиационных исследований Университета г. Упсалы.

1. INTRODUCTION

In our work [1] we investigated mass surface and some properties of nuclei close to neutron-rich nuclide ^{78}Ni offering the astrophysical interest. The mentioned work used two different approaches. The first one consisted in applying the multiparticle shell model that used the mean field and residual interaction with parameters defined from description of nuclear structure in the regions of less neutron excess or in stable nuclei. The second approach was

[1]St.Petersburg Nuclear Physics Institute, Russian Academy of Sciences, Gatchina 188300, Russia
[2]Physicotechnical Institute, Russian Academy of Sciences, St.Petersburg 194021, Russia
[3]Department of Radiation Sciences, Uppsala University, Nyköping S-61162, Sweden

based on resemblance of the shell structure of ^{78}Ni and that of ^{132}Sn. The latter doubly magic nuclide is actively investigated at the present time [2,3]. Such resemblance was first observed by Blomqvist [4], but conformably to the pair of nuclei — ^{132}Sn and ^{208}Pb. It was noted by us in [1] that the known so far as well as not yet well investigated (or even not yet discovered) regions of magicity, in the sence of resemblance of nuclear structure, may be considered as lying in the (Z, N) coordinates on two axes, one leading to neutron excess, while another one — to neutron deficient nuclei. Among the least, one may mention the nuclides in the vicinity of ^{100}Sn, also hardly studied so far (see for example [5–10] and the references therein) as well as nuclei close to $Z = N = 82$, about which any experimental information is absent by now.

The investigation of both mass regions ($A \approx 100$ and $A \approx 164$) is of great importance because it can shed light on the problem of «universality» of nucleon magic numbers throughout the Chart of nuclides. The question whether this universality is fulfilled in the mass regions very far off the β-stability line has a principal meaning. Especially, it is interesting to learn whether the magic properties of the ^{164}Pb nuclide, which is situated beyond and far from the proton drip-line, can provide the existence of the island of quasi-stability in the sea of full nucleon instability of nuclides.

The problem of universality which was formulated long time ago [11] is still under discussion [12, 13]. Meanwhile the interest to the hypothetic magic nuclides should be increased nowadays in connection with the advent of Radioactive Ion Beam facilities which main goals are just concentrated on the production and investigation of exotic nuclides. To prepare some guide for the future experiments we have carried out the evaluation of the expected properties of the mentioned nuclides.

Thus the aim of the present paper is to obtain some theoretical estimates on the properties of nuclides utmost remote from the β-stability line, which are evidently unstable to the proton decay. The calculations for the magic region of light lead were held in the framework of two microscopical and partially overlapping approaches, one of which is based on the multiparticle shell model [14], whereas the other — on the self consistent procedure of Hartree–Fock, accounting for pairing correlations (HF+BCS; see, for example, [15–18]).

2. CALCULATIONS OF THE MASS SURFACE OF NUCLEI CLOSE TO ^{164}Pb USING THE MULTIPARTICLE SHELL MODEL

The shell-model calculations presented in this work are based on the concepts of nuclear mean field and residual interaction. The parameters of the mean field potential of the Woods-Saxon type were fitted by us from the comparison with the experimental data on single-particle energies for nuclei close to ^{208}Pb and ^{132}Sn. The finite range effective interaction used by us here was applied earlier for the description of «two-quasiparticle» nuclei around the magic cores [19–23].

Another basic idea consists in using the ground state of ^{164}Pb as a vacuum relatively to which all near-magic nuclei can be considered as few quasiparticle ones. This consideration in practice includes all the nuclei having proton and neutron numbers in the interval $80 \leq Z, N \leq 84$ (totally 25 cases studied by us here).

Let us consider the Hamiltonian in the Hartree–Fock representation which in this case has the form:

$$H = E_0 + \sum_{\alpha} \varepsilon_\alpha N(a^+_\alpha a_\alpha) + \frac{1}{4} \sum_{\alpha,\beta,\gamma,\delta} {}_a\langle\alpha\beta|\vartheta|\gamma\delta\rangle_a \, N(a^+_\alpha a^+_\beta a_\delta a_\gamma), \tag{1}$$

where the single-particle orbitals $|\alpha\rangle$ are formally determined from the self-consistent procedure of the Hartree–Fock type for the core nucleus. In Eq.(1) E_0 is a vacuum energy (binding energy of a ^{164}Pb core with the opposite sign) which is not essential in the case of decay energy determinations, ϑ is the residual interaction and $N(\cdots)$ means a normal (relatively to the assumed vacuum) product of operators.

In reality, for generating single particle orbitals we used Woods–Saxon potential (instead of Hartree–Fock) of the form

$$U(r,\hat{\sigma}) = \frac{V}{1+\exp\left[(r-R)/a\right]} + V_{\ell s} r_0^2 \frac{1}{r}\frac{d}{dr}\left[\frac{1}{1+\exp\left[(r-R)/a\right]}\right] \widehat{\boldsymbol{\ell}} \cdot \widehat{\mathbf{s}}, \tag{2}$$

where $V = -V_0(1 - \beta\frac{N-Z}{A}t_z)$, $R = r_0 A^{1/3}$, $t_z = -1/2$ for p and $t_z = +1/2$ for n (for protons the potential of the uniformly charged sphere with radius $R_c = r_{oc}A^{1/3}$ was added).

We performed calculations using three different sets of parameters entering Eq. (2). Potential $Stnd$ was borrowed from the works [19–23] and had the following values of parameters: $V_0 = 51.5$ MeV, $r_0 = 1.27$ fm, $\beta = 1.39$, $V_{\ell s} = -0.43\,V$, $r_{oc} = 1.25$ fm. The effective diffuseness parameters a for protons and neutrons were chosen to be: $a_p = 0.67$ fm and $a_n = 0.55$ fm, where index «p» refers to protons, while «n» — to neutrons. Potential $Set3$ was defined by us in [24] and gives the best description of single-particle spectra in the region of ^{100}Sn. At the same time, the BEn potential gives an adequate description of the single particle separation energies in the chain of isotopes from ^{132}Sn to ^{100}Sn. Our effective interaction has the form:

$$\vartheta = (V + V_\sigma \boldsymbol{\sigma}_1\boldsymbol{\sigma}_2 + V_T S_{12} + V_\tau \boldsymbol{\tau}_1\boldsymbol{\tau}_2 + V_{\sigma\tau}\boldsymbol{\sigma}_1\boldsymbol{\sigma}_2\cdot\boldsymbol{\tau}_1\boldsymbol{\tau}_2 + V_{\tau T}S_{12}\boldsymbol{\tau}_1\boldsymbol{\tau}_2)\exp\left(-\frac{r^2}{r_{00}^2}\right) \tag{3}$$

with $V = -9.95$, $V_\sigma = 2.88$, $V_T = -1.47$, $V_\tau = 5.90$, $V_{\sigma\tau} = 4.91$, $V_{\tau T} = 1.51$ MeV and $r_{00} = 1.8$ fm.

Single-particle energies generated by the potential (2) were used to define the binding energies for four odd-mass nuclei adjacent to ^{164}Pb as well as to generate the whole single-particle spectrum which is necessary for calculations of binding energies for nuclides having more than one quasiparticle (where the residual interaction between the nucleons as well as configuration mixing are essential).

Let us consider separately different cases arising for nuclides with more than one valence quasiparticle:

2.1. The Nuclides of the Type «^{164}Pb Core Plus Two Quasiparticles». Ground state binding energies were obtained from the RPA-calculations, with the eigenfrequencies and amplitudes of states $f_{\alpha\beta} = \binom{X}{Y}$ defined by systems of equations that have the following form in a matrix notation:

$$\begin{Vmatrix} A & M \\ M & C \end{Vmatrix} \begin{pmatrix} X \\ Y \end{pmatrix} = \omega_k \begin{pmatrix} X \\ -Y \end{pmatrix} \tag{4}$$

with the normalization condition

$$\left| \sum_{\alpha,\beta} X_{\alpha\beta}(\omega_k) X_{\alpha\beta}(\omega_{k'}) - \sum_{\alpha,\beta} Y_{\alpha\beta}(\omega_k) Y_{\alpha\beta}(\omega_{k'}) \right| = \delta(kk'), \tag{5}$$

where $f_{\alpha\beta} = \binom{X_{ab}}{Y_{a'b'}}$ for particle–particle (nuclides of the type «core $\pm 2p, \pm 2n$, $\pm p \pm n$») and $f_{\alpha\beta} = \binom{X_{ab'}}{Y_{a'b}}$ for particle-hole (nuclides of the type «core $\pm p \mp n$») channels. Latin indices with and without primes refer to states below and above the Fermi levels, respectively.
The expressions in equation (4) stand for the following:

$$A_{\alpha\beta;\mu\nu} = E_{\alpha\beta}\delta_{\alpha\mu}\delta_{\beta\nu} + M^J_{\alpha\beta;\mu\nu} \tag{6}$$

$$C_{\alpha\beta;\mu\nu} = -E_{\alpha\beta}\delta_{\alpha\mu}\delta_{\beta\nu} + M^J_{\alpha\beta;\mu\nu}. \tag{7}$$

For the particle-particle channel $E_{\alpha\beta} = \varepsilon_\alpha + \varepsilon_\beta$; $\alpha = a$, $\beta = b$ (or $\alpha = a'$, $\beta = b'$) and $M^J_{\alpha\beta;\mu\nu}$ is a properly antisymmetrized particle-particle matrix element between the states $|\alpha\beta; J>$ and $|\mu\nu; J>$ with a given value of angular momenta. For the particle-hole channel $E_{\alpha\beta} = \varepsilon_\alpha - \varepsilon_\beta$; $\alpha = a$, $\beta = b'$ (or $\alpha = a'$, $\beta = b$) and $M^J_{\alpha\beta;\mu\nu}$ is a particle-hole matrix element. The formulae for particle-particle and particle-hole matrix elements $M^J_{\alpha\beta;\mu\nu}$ one may see in [19, 20]. The «upper» solutions having $\omega_n \simeq \varepsilon_a + \varepsilon_b$ for the particle-particle channel correspond to the $(A+2)$, while the «lower» ones, with $\omega_m \simeq \varepsilon'_a + \varepsilon'_b$ correspond to the $(A-2)$ nuclides. In this case the solutions ω of the system (4) are related to the excitation energies by equations:

$$E_n(A+2) = \omega_n + B(A+2) - B(A), \tag{8}$$

$$E_m(A-2) = -\omega_m + B(A-2) - B(A), \tag{9}$$

where $B(A)$ and $B(A+2)$ present the ground state binding energies and A refers to the core ($B(A) \equiv -E_0(A)$). For the charged particle-hole channel $\omega_n \simeq \varepsilon_a - \varepsilon'_b$ corresponds to the «core $+p-n$», while $\omega_m \simeq \varepsilon'_a - \varepsilon_b$ – to the «core $-p+n$» nuclides. Here we have:

$$E_n(Z+1, N-1) = \omega_n + B(Z+1, N-1) - B(Z, N), \tag{10}$$

$$E_m(Z-1, N+1) = -\omega_m + B(Z-1, N+1) - B(Z, N), \tag{11}$$

where Z, N refer to the core. The differences of binding energies $B(A \pm 2) - B(A)$ and $B(Z \pm 1, N \mp 1) - B(A)$ between the two quasiparticle states and the core nuclei were defined by variation of the $B(A \pm 2)$ and $B(Z \pm 1, N \mp 1)$ values until the excitation energies E_n and E_m of the lowest states as defined by (8)–(11) become equal to zero.

2.2. The Nuclides of the Type «^{164}Pb Core Plus Three Quasiparticles». The nuclei considered by us here have a structure of the types «core$\pm 2p \pm n$, $\pm 2p \mp n$, $\pm 2n \pm p$, and $\pm 2n \mp p$». In all these cases the calculations have been performed in the framework of the three quasiparticle shell model and the wave function was expressed as follows:

$$\Psi_{IM} = \sum_{\alpha,\beta,\mu,J} X^I_{\alpha\mu(J)\beta} \left| \left[\xi^+_{j_\alpha} \xi^+_{j_\mu} \right]^J, \xi^+_{j_\beta}; IM \right| 0\rangle \tag{12}$$

with

$$[\xi^+_{j_\alpha}\xi^+_{j_\mu}]^{JM} = \frac{1}{\sqrt{1+\delta_{j_\alpha j_\mu}}}\sum_{m_\alpha,m_\mu} C^{JM}_{j_\alpha m_\alpha j_\mu m_\mu}\xi^+_{j_\alpha m_\alpha}\xi^+_{j_\mu m_\mu} \tag{13}$$

and

$$\xi^+_{j_a m_a} = a^+_{j_a m_a};\ \xi^+_{j_{a'} m_{a'}} = (-1)^{\ell_{a'}+j_{a'}-m_{a'}}a_{j_{a'}-m_{a'}}. \tag{14}$$

In (12) $\alpha,\mu \in p,\ \beta \in n$ or $\alpha,\mu \in n,\ \beta \in p$ (α,μ simultaneously belong to particles or holes), $|0\rangle$ is a ground state wave function of ^{164}Pb. The eigenvectors (X) and the eigenstates were obtained by solving the secular equation:

$$\|D\| \cdot (X) = \omega_k(X) \tag{15}$$

with

$$\begin{aligned} D^{J_2J_1(I)}_{\alpha_2\mu_2\beta_2,\alpha_1\mu_1\beta_1} &= (\bar\varepsilon_{\alpha_1}+\bar\varepsilon_{\mu_1}+\bar\varepsilon_{\beta_1})\delta_{\alpha_2\alpha_1}\delta_{\mu_2\mu_1}\delta_{\beta_2\beta_1}\delta_{J_2J_1} \\ &+ \langle\alpha_2\mu_2(J_2)\beta_2;I|H_{int}|\alpha_1\mu_1(J_1)\beta_1;I\rangle, \end{aligned} \tag{16}$$

where $\bar\varepsilon_a = \varepsilon_a, \bar\varepsilon_{a'} = -\varepsilon_{a'}$, etc., and the excitation energies E_k are connected with ω_k in Eq. (15) by the relation:

$$E_k = \omega_k + B(A+3qp) - B(A). \tag{17}$$

The three quasiparticle interaction matrix element in (16) can be expressed via M^J-values:

$$\langle\alpha_2\mu_2(J_2)\beta_2;I|H_{int}|\alpha_1\mu_1(J_1)\beta_1;I\rangle = \delta_{\beta_2\beta_1}\delta_{J_2J_1}M^{J_1}_{\alpha_2\mu_2;\alpha_1\mu_1} +$$

$$+\left[\frac{(2J_2+1)(2J_1+1)}{(1+\delta_{\alpha_2\mu_2})(1+\delta_{\alpha_1\mu_1})}\right]^{1/2}\Bigg\{\delta_{\mu_2\mu_1}\sum_L(2L+1)W[j_{\beta_2}LJ_2j_{\mu_2};j_{\alpha_2}I]W[j_{\beta_1}LJ_1j_{\mu_2};j_{\alpha_1}I]$$

$$\times M^L_{\alpha_2\beta_2;\alpha_1\beta_1} + (-1)^{j_{\alpha_1}+j_{\mu_1}+J_1+1}\delta_{\mu_2\alpha_1}\sum_L(2L+1)W[j_{\beta_2}LJ_2j_{\mu_2};j_{\alpha_2}I]W[j_{\beta_1}LJ_1j_{\mu_2};j_{\mu_1}I]$$

$$\times M^L_{\alpha_2\beta_2;\mu_1\beta_1} + (-1)^{j_{\alpha_2}+j_{\mu_2}+J_2+1}\delta_{\alpha_2\mu_1}\sum_L(2L+1)W[j_{\beta_2}LJ_2j_{\alpha_2};j_{\mu_2}I]W[j_{\beta_1}LJ_1j_{\alpha_2};j_{\alpha_1}I]$$

$$\times M^L_{\mu_2\beta_2;\alpha_1\beta_1} + (+1)^{j_{\alpha_2}+j_{\mu_2}+J_2+j_{\alpha_1}+j_{\mu_1}+J_1}\delta_{\alpha_2\alpha_1}\times$$

$$\times\ \sum_L(2L+1)W[j_{\beta_2}LJ_2j_{\alpha_2};j_{\mu_2}I]W[j_{\beta_1}LJ_1j_{\alpha_2};j_{\mu_1}I]M^L_{\mu_2\beta_2;\mu_1\beta_1}\Bigg\}. \tag{18}$$

In Eq. (18) and below $M^J_{ab;cd}$ and $M^J_{a'b';c'd'}$ refer to particle-particle, while $M^J_{ab';cd'}$ and $M^J_{a'b;c'd}$ refer to particle-hole channels.

The values of $B(A+3qp)$ are determined by the condition that the energy E_k of the lowest level is equal to zero.

Table 1. Mass surface in the neighborhood of ^{164}Pb

Z						
84		^{164}Po; 0^+	^{165}Po; $1/2^+$	^{166}Po; 0^+	^{167}Po; $9/2^-$	^{168}Po; 0^+
	a)	$-48.99(1.15)$	$-31.88(1.09)$	$-13.34(0.84)$	$0.26(0.94)$	$14.27(1.05)$
	b)	-49.84	-32.62	-14.70	-2.14	11.95
		^{163}Bi; $9/2^-$	^{164}Bi; 4^-	^{165}Bi; $9/2^-$	^{166}Bi; $1^+(0^+)$	^{167}Bi; $9/2^-$
83	a)	$-42.04(0.87)$	$-25.09(0.63)$	$-7.24(0.44)$	$7.08(0.46)$	$20.52(0.90)$
	b)	-42.00	-25.48	-7.66	$5.50; 9^+(1^+, 0^+)$	18.20
		^{162}Pb; 0^+	^{163}Pb; $1/2^+$	^{164}Pb; 0^+	^{165}Pb; $9/2^-$	^{166}Pb; 0^+
82	a)	$-33.89(0.67)$	$-17.64(0.34)$		$12.87(0.43)$	$27.06(0.83)$
	b)	-33.63	-17.34		11.85	24.85
		^{161}Tl; $1/2^+$	^{162}Tl; 1^+	^{163}Tl; $1/2^+$	^{164}Tl; 4^-	^{165}Tl; $1/2^+$
81	a)	$-28.92(0.45)$	$-12.90(0.11)$	$3.15(0.24)$	$15.89(0.65)$	$29.36(1.10)$
	b)	-30.54	-13.09	2.74	14.12	27.22
		^{160}Hg; 0^+	^{161}Hg; $1/2^+$	^{162}Hg; 0^+	^{163}Hg; $9/2^-$	^{164}Hg; 0^+
80	a)	$-23.26(0.20)$	$-8.41(0.12)$	$7.16(0.46)$	$19.43(0.87)$	$32.70(1.30)$
	b)	-27.01	-10.82	5.83	17.02	29.62
		80	81	82	83	84 N

The values of $B(Z,N) - B(^{164}\mathrm{Pb})$ in the multiparticle shell-model, with averaging over the mean field potential, are presented in lines «a»; numbers in brackets are the dispersions of the averaging procedure, σ. The results of the HF+BCS calculations are presented in lines «b». The differences of energies are calculated with $m_n \neq m_p$. In this case $B(^{164}\mathrm{Pb}) = 1200.3$ MeV. If one takes $m_n = m_p \equiv m_n$ then $B(^{164}\mathrm{Pb})$ is equal to 1202.3 MeV, while the $B(Z,N) - B(^{164}\mathrm{Pb})$ values change very small, by the numbers not more than ~ 0.05 MeV.

Table 2. Averaged decay energies in the vicinity of ^{164}Pb, calculated in the multiparticle shell-model

Nucleus	$Q_{\beta+}$	Q_p	Q_{2p}	Q_α
$^{168}_{84}\mathrm{Po}_{84}$	—	6.25(1.38)	12.79(1.34)	14.03(1.05)
$^{167}_{84}\mathrm{Po}_{83}$	18.45(1.30)	6.82(1.05)	12.61(1.03)	10.40(1.00)
$^{166}_{84}\mathrm{Po}_{82}$	18.61(0.92)	6.10(0.95)	13.34(0.84)	7.75(1.07)
$^{165}_{84}\mathrm{Po}_{81}$	23.19(1.17)	6.79(1.26)	14.24(1.14)	–
$^{164}_{84}\mathrm{Po}_{80}$	22.09(1.31)	6.95(1.44)	15.10(1.33)	–
$^{167}_{83}\mathrm{Bi}_{84}$	—	6.54(1.22)	8.84(1.42)	10.93(0.93)
$^{166}_{83}\mathrm{Bi}_{83}$	18.17(0.95)	5.79(0.63)	8.81(0.80)	8.32(0.47)
$^{165}_{83}\mathrm{Bi}_{82}$	18.31(0.61)	7.24(0.44)	10.39(0.50)	6.62(0.63)
$^{164}_{83}\mathrm{Bi}_{81}$	23.28(0.63)	7.45(0.72)	12.19(0.64)	–
$^{163}_{83}\mathrm{Bi}_{80}$	22.59(0.93)	8.15(1.10)	13.12(0.98)	–
$^{166}_{82}\mathrm{Pb}_{84}$	—	2.30(1.38)	5.64(1.54)	8.40(0.95)
$^{165}_{82}\mathrm{Pb}_{83}$	14.68(1.18)	3.02(0.78)	6.56(0.97)	7.02(0.45)
$^{164}_{82}\mathrm{Pb}_{82}$	14.08(0.65)	3.15(0.24)	7.16(0.46)	5.04(0.20)
$^{163}_{82}\mathrm{Pb}_{81}$	18.98(0.42)	4.76(0.36)	9.23(0.36)	–
$^{162}_{82}\mathrm{Pb}_{80}$	19.18(0.68)	4.97(0.81)	10.63(0.70)	–
$^{165}_{81}\mathrm{Tl}_{84}$	–	3.34(1.70)	–	–
$^{164}_{81}\mathrm{Tl}_{83}$	15.00(1.45)	3.54(1.09)	–	–
$^{163}_{81}\mathrm{Tl}_{82}$	14.47(0.90)	4.01(0.52)	–	–
$^{162}_{81}\mathrm{Tl}_{81}$	18.25(0.47)	4.49(0.16)	–	–
$^{161}_{81}\mathrm{Tl}_{80}$	18.70(0.47)	5.66(0.49)	–	–

Root mean square errors of the Q values correspond to the «errors» σ of binding energies of the initial and final states, that are pointed in Table 1.

Table 3. Decay energies of nuclei close to ^{164}Pb, calculated in the framework of the HF+BCS method

Nucleus	$Q_{\beta+}$	Q_p	Q_{2p}	Q_α
^{168}Po	—	6.25	12.90	16.35
^{167}Po	18.53	7.64	13.99	13.10
^{166}Po	18.39	7.04	14.70	9.37
^{165}Po	23.15	7.14	15.28	–
^{164}Po	22.55	7.84	16.21	–
^{167}Bi	—	6.65	9.02	12.84
^{166}Bi	17.54	6.35	8.62	9.71
^{165}Bi	17.70	7.66	10.40	5.42
^{164}Bi	23.67	8.14	12.39	–
^{163}Bi	22.85	8.37	11.46	–
^{166}Pb	—	2.37	4.77	9.28
^{165}Pb	13.56	2.27	5.17	5.63
^{164}Pb	12.31	2.74	5.83	1.29
^{163}Pb	18.27	4.25	6.52	–
^{162}Pb	18.73	3.09	6.62	–
^{165}Tl	—	2.40	—	—
^{164}Tl	13.69	2.90	—	—
^{163}Tl	12.47	3.09	—	—
^{162}Tl	17.11	2.27	—	—
^{161}Tl	17.91	3.53	—	—

In composing this Table the Skyrme III interaction and $G_p = 23/A$ MeV, $G_n = 21/A$ MeV values of the pairing constants are used.

2.3. The Nuclides of the Type «^{164}Pb Plus Four Quasiparticles». These nuclides have a structure «core$\pm 2p \pm 2n$ and $\pm 2p \mp 2n$». The wave function can be written in this case as follows:

$$\Psi_{IM} = \sum_{\alpha,\mu,\beta,\eta,J_1,J_2} X^I_{\alpha\mu(J_1)\beta\eta(J_2)} |[\xi^+_{j\alpha}\xi^+_{j\mu}]^{J_1}, [\xi^+_{j\beta}\xi^+_{j\eta}]^{J_2}; IM|0\rangle \tag{19}$$

with $\alpha, \mu \in p,\ \beta, \eta \in n$ or $\alpha, \mu \in n,\quad \beta, \eta \in p$ and $\alpha\mu$ or $\beta\eta$ simultaneously belong to particles or holes. In practical calculations we used in the basis only the functions with $J_1 = J_2 = 0$ giving the greatest matrix elements of interaction within the $I = 0$ basis states. In this case $\alpha = \mu,\ \beta = \eta$ and the corresponding secular equation formally also has the form (15) with

$$\begin{aligned} D_{\alpha_2\beta_2,\alpha_1\beta_1} &= (2\bar{\varepsilon}_{\alpha_2} + 2\bar{\varepsilon}_{\beta_2})\delta_{\alpha_2\alpha_1}\delta_{\beta_2\beta_1} + \delta_{\beta_2\beta_1} M^0_{\alpha_2\alpha_2,\alpha_1\alpha_1} + \delta_{\alpha_2\alpha_1} M^0_{\beta_2\beta_2,\beta_1\beta_1} \\ &+ \delta_{\alpha_2\alpha_1}\delta_{\beta_2\beta_1} \frac{4}{(2j_{\alpha_1}+1)(2j_{\beta_1}+1)} \sum_L (2L+1) M^L_{\alpha_1\beta_1,\alpha_1\beta_1}. \end{aligned} \tag{20}$$

The single-particle basis that includes all single-particle states of corresponding valence shells was used for all two-, three- and four-quasiparticle nuclides.

Table 1 (lines «a») presents the calculated differences of binding energies, $B(A) - -B(^{164}\mathrm{Pb})$. The predicted values of the ground state spins are also presented in this Table. The values of one- and two-proton separation energies, as well as β- and α-decay energies are presented in Table 2. One should mention that the procedure for definition of $B(A) - B(^{164}\mathrm{Pb})$ values, based on the shell-model approach that uses the same vacuum for all the nuclei studied by us, does not take into account the rearrangement effects (see the discussion below).

3. CALCULATIONS USING THE SELF CONSISTENT APPROACH

As the nuclei considered by us here are extremely neutron-deficient, long extrapolations of the phenomenological parameters defining the mean field and residual interaction may be rather speculative. Below we consider the problem of the mass surface in the vicinity of ^{164}Pb in the framework of another method, namely the HF+BCS approximation using the Skyrme III interaction and the constant pairing theory to account the pairing correlations. In this case the total energy E has the form (see also [15–18]):

$$E \;=\; 4\pi \int_0^\infty H(r) r^2 dr - \frac{\Delta_p^2}{G_p} - \frac{\Delta_n^2}{G_n}\;, \tag{21}$$

where

$$\begin{aligned} H(r) \;&=\; \frac{A-1}{A}\left[\frac{\hbar^2}{2m_p}\,\tau_p + \frac{\hbar^2}{2m_n}\,\tau_n\right] + \frac{t_0}{2}\left[\left(1+\frac{x_0}{2}\right)\rho^2 - \left(x_0+\frac{1}{2}\right)\left(\rho_p^2+\rho_n^2\right)\right] + \\ &+\; \frac{1}{4}(t_1+t_2)\rho\tau + \frac{1}{8}(t_2-t_1)(\rho_n\tau_n+\rho_p\tau_p) + \frac{1}{4}\,t_3\rho\rho_n\rho_p + \\ &+\; \frac{1}{32}(3t_1+t_2)\left[\rho_n\left(\frac{d^2\rho_n}{dr^2}+\frac{2}{r}\frac{d\rho_n}{dr}\right)+\rho_p\left(\frac{d^2\rho_p}{dr^2}+\frac{2}{r}\frac{d\rho_p}{dr}\right)\right] + \\ &+\; \frac{1}{16}(t_2-3t_1)\rho\left(\frac{d^2\rho}{dr^2}+\frac{2}{r}\frac{d\rho}{dr}\right) + \frac{1}{16}(t_1-t_2)\left(J_n^2+J_p^2\right) - \\ &-\; \frac{1}{2}W_0\left[\rho\left(\frac{dJ}{dr}+\frac{2}{r}\,J\right)+\rho_n\left(\frac{dJ_n}{dr}+\frac{2}{r}\,J_n\right)+\rho_p\left(\frac{dJ_p}{dr}+\frac{2}{r}\,J_p\right)\right] + \\ &+\; 2\pi e^2\rho_p\left[\frac{1}{r}\int_0^r \rho_p(x)x^2dx + \int_r^\infty \rho_p(x)xdx\right] - \frac{3}{4}\left(\frac{3}{\pi}\right)^{1/3} e^2\rho_p^{4/3}\;. \end{aligned} \tag{22}$$

In formula (22) we subtracted (in the single particle approximation) the center of mass motion and took into account the exchange Coulomb energy in the Slater approach. The quantities t_0, t_1, t_2, t_3, x_0 and W_0 entering (22) are the Skyrme III parameters [17], while the expressions for the density of matter as well as for kinetic energy and spin densities have the form:

$$\rho_q(r) \;=\; \frac{1}{4\pi r^2}\sum_\alpha\; v_{q,\alpha}^2(2j_{q,\alpha}+1)\;R_{q,\alpha}^2\;; \tag{23}$$

$$\tau_q(r) = \frac{1}{4\pi r^2}\sum_\alpha v_{q,\alpha}^2(2j_{q,\alpha}+1)\left[\left(\frac{dR_{q,\alpha}}{dr}\right)^2 + \frac{\ell(\ell+1)+1}{r^2}R_{q,\alpha}^2 - \frac{2}{r}R_{q,\alpha}\cdot\frac{dR_{q,\alpha}}{dr}\right]; \tag{24}$$

$$J_q(r) \;=\; \frac{1}{4\pi r^3}\sum_\alpha v_{q,\alpha}^2(2j_{q,\alpha}+1)\left[j_{q,\alpha}(j_{q,\alpha}+1) - \ell_{q,\alpha}(\ell_{q,\alpha}+1) - \frac{3}{4}\right]R_{q,\alpha}^2, \tag{25}$$

where $q = p$, or n; $\rho = \rho_p + \rho_n$, $\tau = \tau_p + \tau_n$, $J = J_p + J_n$.

Radial wave functions $R_{q\alpha}(r)$ entering the densities are normalized by the condition $\int_0^\infty R^2 dr = 1$ and are defined by the system of equations

$$R''_{q,\alpha}(r) = \frac{2m_q^*}{\hbar^2}\left\{-\left[\frac{1}{4}(t_1+t_2)\frac{d\rho}{dr}+\frac{1}{8}(t_2-t_1)\frac{d\rho_q}{dr}\right]R'_{q,\alpha} + (F_{q,\alpha}-\varepsilon_{q,\alpha})R_{q,\alpha}\right\}, \tag{26}$$

where

$$\begin{aligned}
F_{q,\alpha} &= t_0\Big[\Big(1+\frac{x_0}{2}\Big)\rho-\Big(x_0+\frac{1}{2}\Big)\rho_q\Big]+\frac{1}{4}t_3(\rho^2-\rho_q^2)\ - \\
&- \frac{1}{8}(3t_1-t_2)\Big[\frac{d^2\rho}{dr^2}+\frac{2}{r}\frac{d\rho}{dr}\Big]+\frac{1}{16}(3t_1+t_2)\Big[\frac{d^2\rho_q}{dr^2}+\frac{2}{r}\frac{d\rho_q}{dr}\Big]+ \\
&+ \frac{1}{r}\Big[\frac{1}{4}(t_1+t_2)\frac{d\rho}{dr}+\frac{1}{8}(t_1-t_2)\frac{d\rho_q}{dr}\Big]+\frac{1}{4}(t_1+t_2)\tau+\frac{1}{8}(t_2-t_1)\tau_q\ - \\
&- \frac{1}{2}W_0\Big[\frac{d(J+J_q)}{dr}+\frac{2}{r}(J+J_q)\Big]+\frac{\hbar^2}{2m_q^*}\ \frac{\ell(\ell+1)}{r^2}\quad + \\
&+ \frac{1}{r}\Big[\frac{1}{2}W_0\frac{d(\rho+\rho_q)}{dr}+\frac{1}{8}(t_1-t_2)J_q\Big]\Big[j(j+1)-\ell(\ell+1)-\frac{3}{4}\Big]\ + \\
&+ \Big[4\pi e^2\Big(\frac{1}{r}\int\limits_0^r\rho_p(x)x^2dx+\int\limits_r^\infty\rho_p(x)xdx\Big)-\Big(\frac{3}{\pi}\Big)^{1/3}e^2\rho_p^{1/3}\Big]\cdot\delta_{pq}\ . \qquad (27)
\end{aligned}$$

In formulas (26), (27)

$$\Big(\frac{m_q}{m_q^*}\Big)\ =\ \frac{A-1}{A}+\Big[\frac{1}{4}(t_1+t_2)\rho+\frac{1}{8}(t_2-t_1)\rho_q\Big]\cdot\frac{2m_q}{\hbar^2}\ . \qquad (28)$$

The $v_{q,\alpha}^2$ quantities entering equations (23)–(25) present the occupancies of the (q,α) orbitals and are defined from the self consistent, together with equations (26), procedure that uses in the pairing channel the constant pairing approximation:

$$\begin{aligned}
v_{q,\alpha}^2 &= \frac{1}{2}\Big(1-\frac{\varepsilon_{q,\alpha}-\lambda_q}{\sqrt{(\varepsilon_{q,\alpha}-\lambda_q)^2+\Delta_q^2}}\Big),\quad u_{q,\alpha}^2=1-v_{q,\alpha}^2\ , \\
1 &= \frac{G_q}{4}\sum_\alpha\frac{(2j_{q,\alpha}+1)}{\sqrt{(\varepsilon_{q,\alpha}-\lambda_q)^2+\Delta_q^2}}\ ,\quad N_q=\sum_\alpha(2j_{q,\alpha}+1)v_{q,\alpha}^2\ ; \qquad (29)
\end{aligned}$$

$N_p=Z$, $N_n=N$, where $\varepsilon_{q,\alpha}$ are defined by the system (26).

For joint solution of systems (26), (29) the iteration procedure was employed. As starting ones, the eigenfunctions R, single particle energies ε and occupancies v^2 for the appropriate Woods–Saxon potential were used. They were employed for the calculation of the right–hand parts of equations (26) that define new values of R,ε, and then, using (29), – the v^2 quantities. Then the procedure was reiterated to achieve the necessary precision.

The method employed for definition of eigenvalues ε allowed us to find eigenvalues both for bound (with $\varepsilon<0$) and unbound ($\varepsilon>0$), but sub-barrier (quasi-stationary) states. In the last case the shell-model function of a quasi-stationary state is defined and normalized to unity in the interval from $r=0$ up to the value $r_>$, corresponding to the external turning point, which position in case of protons is defined as:

$$r_>(fm)\ \approx\ 0.72\frac{Z}{\varepsilon}\ \delta_{pq}+\sqrt{0.518\Big(\frac{Z}{\varepsilon}\Big)^2\delta_{pq}+20.7\frac{A-1}{A}\cdot\frac{\ell(\ell+1)}{\varepsilon}}\ , \qquad (30)$$

where the energy ε is in MeV.

The consideration of the quasi-stationary states equally with the levels having $\varepsilon < 0$, presented by us above, is valid in the case if single particle decay widths of such states are essentially less than the typical nuclear energies. As we shall see further, this condition is fulfilled practically for all the proton quasi-stationary states in nuclei close to ^{164}Pb, except, maybe, the most upper ones.

Table 4. Single-particle energies in ^{164}Pb, calculated in the framework of self-consistent procedure with the Skyrme III interaction

Protons		Neutrons	
$n\,\ell\,j$	$\varepsilon_{n\ell j}$, MeV	$n\,\ell\,j$	$\varepsilon_{n\ell j}$, MeV
$3p1/2$	12.17	$3p1/2$	-6.46
$3p3/2$	11.42	$3p3/2$	-7.41
$2f5/2$	11.23	$2f5/2$	-7.84
$1i13/2$	9.91	$1i3/2$	-9.21
$2f7/2$	8.88	$2f7/2$	-10.66
$1h9/2$	7.96	$1h9/2$	-11.42
$3s1/2$	3.09	$3s1/2$	-17.08
$2d3/2$	2.30	$2d3/2$	-17.75
$1h11/2$	1.39	$1h11/2$	-18.10
$2d5/2$	0.31	$2d5/2$	-19.90
$1g7/2$	-2.18	$1g7/2$	-21.97
$1g9/2$	-6.84	$1g9/2$	-26.65
$2p1/2$	-7.27	$2p1/2$	-27.82
$2p3/2$	-8.42	$2p3/2$	-29.04
$1f5/2$	-11.74	$1f5/2$	-31.86
$1f7/2$	-14.65	$1f7/2$	-34.76
$2s1/2$	-17.09	$2s1/2$	-38.01
$1d3/2$	-20.31	$1d3/2$	-40.75
$1d5/2$	-21.84	$1d5/2$	-42.27
$1p1/2$	-27.54	$1p1/2$	-48.31
$1p3/2$	-28.15	$1p3/2$	-48.91
$1s1/2$	-33.17	$1s1/2$	-54.32

Results of self consistent calculations of the binding energies are also presented in Table 1 (lines «b»). The BCS procedure used single-particle basis including one shell above and the other – below the proton and neutron Fermi energies. The more deep single-particle states were supposed as completely filled; v^2=1. In the cases of odd–odd ^{166}Bi and ^{162}Tl nuclei the corresponding diagonal particle–particle matrix elements (see [20]) and in the cases of ^{164}Bi and ^{164}Tl — diagonal particle-hole matrix elements [20], calculated with the interaction (3), were added to the expression (21) for energy. The calculated self consistent single-particle energies in ^{164}Pb are presented in Table 4. As one can easily see, the mentioned nuclide has distinct characteristics of a magic nucleus. The magnitudes of proton (4.87 MeV) and neutron (5.66 MeV) gaps guarantee the absence of pairing in this nuclide. For comparison Table 5 presents the similar theoretical spectrum, but for the stable isotope ^{208}Pb. Proton and neutron densities in ^{164}Pb are given in Fig. 1. One can see that in the surface region the proton density is some more than that of neutrons and that the mean square radius of proton distribution is also some more than that of neutrons. At the same time, there is no decrease of the proton density in the center of a ^{164}Pb nucleus. The similar picture, but for ^{208}Pb is presented for comparison in Fig. 2.

Table 5. Some of single-particle energies in ^{208}Pb, calculated in self-consistent approach with the Skyrme III interaction

Protons		Neutrons	
$n\,\ell\,j$	$\varepsilon_{n\ell j}$, MeV	$n\,\ell\,j$	$\varepsilon_{n\ell j}$, MeV
$3p1/2$	2.88	$3d3/2$	0.42
$3p3/2$	2.03	$2g7/2$	0.14
$2f5/2$	0.74	$3d5/2$	-0.38
$1i13/2$	-1.53	$4s1/2$	-0.64
$2f7/2$	-1.66	$1j15/2$	-1.93
$1h9/2$	-4.24	$1i11/2$	-2.77
$3s1/2$	-7.33	$2g9/2$	-2.97
$2d3/2$	-8.51	$3p1/2$	-7.13
$1h11/2$	-9.65	$3p3/2$	-8.15
$2d5/2$	-10.28	$2f5/2$	-8.44
$1g7/2$	-13.59	$1i13/2$	-10.21
$1g9/2$	-17.36	$2f7/2$	-11.24
$2p1/2$	-17.64	$1h9/2$	-12.67
$2p3/2$	-18.63	$3s1/2$	-17.04
$1f5/2$	-22.21	$2d3/2$	-17.63
		$1h11/2$	-18.24
		$2d5/2$	-19.61
		$1g7/2$	-22.12

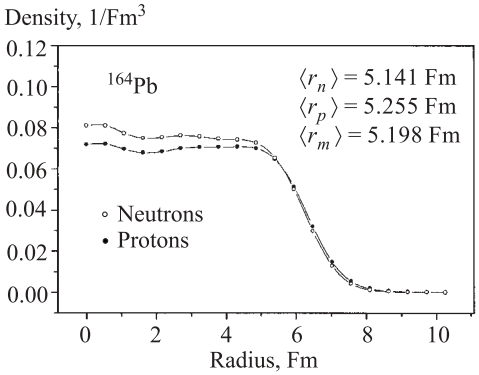

Fig. 1. Proton and neutron densities in ^{164}Pb

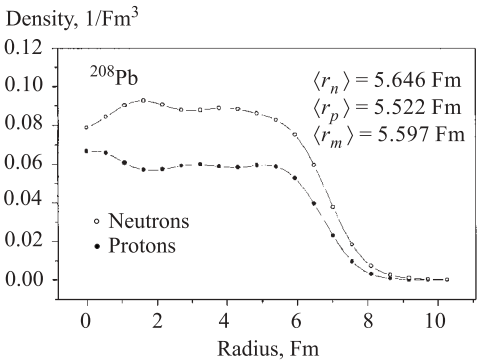

Fig. 2. Proton and neutron densities in ^{208}Pb

The comparison of values of four single-particle nucleon energies closest to proton and neutron gaps and presented among the others in Table 4 with the magnitudes of differences $B(A)-B(\mathrm{core})$ for the ^{165}Pb, ^{165}Bi, ^{163}Bi and ^{163}Tl nuclei (see lines («b») in Table 1) shows that the rearrangement effect arising from the variation of single-particle wave functions with changing the number of nucleons by one unit is not more than 0.4 MeV. This is usually less than the dispersion of the $B(A)-B(\mathrm{core})$ values obtained by us in the shell-model approach and less than the distinction in the mentioned values obtained by two different (shell-model and self-consistent) approaches. This fact presents a justification for using in our shell-model approach of a unique vacuum for all the nuclei considered by us.

4. ON THE STRUCTURE OF ^{164}Pb AND IT'S DECAY PROPERTIES

Here we shall consider the stability of lead-164 relatively to different decay modes.

4.1. Evaluation of Half-Life Relatively to alpha-Decay. For evaluation of the partial half-life $T_{1/2}$ of the ^{164}Pb to α-decay remember the relation $T_{1/2} = 0.693\,\hbar/\Gamma$, where $\Gamma = P \cdot \Gamma_0$, with Γ_0 — the reduced width, and P — the barrier penetrability defined by the formula

$$P \;=\; \exp\left\{-\frac{2}{\hbar}\int\limits_{r_<}^{r_>}\sqrt{2m_\alpha\left[U^\alpha_{\rm opt}(r)+\frac{2(Z-2)e^2}{r}+\frac{\hbar^2\ell(\ell+1)}{2m_\alpha r^2}-\varepsilon\right]}\,dr\right\}, \qquad (31)$$

where ε, m_α and ℓ are the kinetic energy, mass and the angular momentum of the α-particle, $r_<$ and $r_>$ are the turning points while $U^\alpha_{\rm opt}(r)$ is the real part of the α-particle optical potential relating to the daughter nucleus. The main difficulty in defining the absolute value of $T^\alpha_{1/2}$ is associated with calculation of the reduced width Γ_0, which is strongly dependent on nuclear structure. Even in the most advanced calculations [25] that considered α-decay of nuclei near the doubly closed shells, which took into account configuration mixing in the RPA scheme and used the integral approach [26, 27] for description of widths, the obtained theoretical widths were found to be two orders of magnitude less than the experimental ones. The reason of this is that up to now one is unable to take properly into account the continuum states in the particle-particle channel. Therefore here for definition of the $T^\alpha_{1/2}$ for ^{164}Pb we use the indirect method based on the similarity of the α-decay of interest ($0^+ \to 0^+$ transition between the doubly magic nucleus and the nucleus «doubly magic $-2p-2n$») and the $0^+ \to 0^+$ decay of ^{212}Po$(0^+) \to ^{208}$Pb$(0^+) + \alpha$ (transition of the type «doubly magic nuclei $+2p+2n \to$ «doubly magic nuclide») with $Q_\alpha \approx 8.8$ MeV and $T^\alpha_{1/2} = 3.04 \cdot 10^{-7}$ s. Supposing the identity of reduced widths Γ_0 in both cases we thus have the relation

$$T^\alpha_{1/2}(^{164}\mathrm{Pb}) \;=\; T^\alpha_{1/2}(^{212}\mathrm{Po}) \cdot \frac{P(^{212}\mathrm{Po}, Q_\alpha = 8.8\ \mathrm{MeV})}{P(^{164}\mathrm{Pb}, Q_\alpha \approx 5\ \mathrm{MeV})}\ . \qquad (32)$$

In numerical calculations we used α-particle optical potentials from the works [28,29], potential «2BL» from [30], and also rectangular–form nuclear potentials with radii $1.17\,A^{1/3}$ fm and $1.25(A^{1/3}+4^{1/3})$ fm. The obtained values of $T^\alpha_{1/2}(^{164}$Pb) in the case of $Q_\alpha \approx 5$ MeV (the most value of this quantity, presented in Table 2) was found to lie in the interval from 3 to 10 years, with $T^\alpha_{1/2} = 5.2$ years for the potential [28] and 7.3 years for the potential [30]. Due to uncertainty of the Q_α value (compare Tables 2 and 3) our estimate presents rather the lower limit of the half-life.

4.2. Beta-Decay and Some Properties of the $A = 164$ Isobars. To determine the probability of the β^+-decay of ^{164}Pb we must know the structure of isobars with $A = 164$. Here we present some results concerning ^{164}Pb (the magic nuclide) and ^{164}Tl (magic nuclide $-p+n$). The calculations were performed in the framework of the RPA method. One can find the corresponding formulas for the magic nuclei in our work [23], while the calculations for ^{164}Tl correspond to the procedure described by us in [20]; see also formulas (4)–(11) of the present work. In our calculations we used the effective interaction (3) while the single-particle basis included all the proton and neutron single-particle states belonging to the $50 \div 82$ and $82 \div 126$ shells with the energies calculated in the self consistent approach (see Table 4).

Some of the ^{164}Pb and ^{164}Tl levels offering the interest to us are presented in Fig. 3. The lowest levels of ^{164}Tl, in accordance with the structure of the main amplitudes of states, present the components of the particle–hole multiplets, two of which are partially represented in the figure. All the low-lying levels of this nucleus have the values of $(T, T_Z) = (1, 1)$. One can see another picture in ^{164}Pb. Here the ground state and the lowest levels are characterized by the values of $(T, T_Z) = (0, 0)$ with insignificant admixtures having $(T, T_Z) = (1, 0)$. Among the higher lying levels there stand out the ones for which the fraction of components (sum of the squared amplitudes) with $T = 1$ is close to 100%. These levels are the isobaric analogs of the ^{164}Tl states and are characterized approximately by the same, as for ^{164}Tl, energy splitting.

Fermi transitions between the 0^+ ground state of ^{164}Pb and the possible 0^+- excitations of ^{164}Tl are strongly configurationally forbidden. The most like β^+-transition of the ^{164}Pb from it's ground state is of the Gamow–Teller type and proceeds to the 1^+- state of ^{164}Tl with the energy of 3.30 MeV. Our calculation, performed in the framework of the RPA approach with the exact implementation of the «difference sum rule», gives for this transition the magnitude of $\mathrm{B}(GT; 0^+ \to 1^+) = 18.84$. This is slightly less than the diagonal shell model value equal to $240/11 \approx 21.82$, corresponding to the spin-flip $ph_{11/2} \to nh_{9/2}$ $(0^+ \to 1^+)$ Gamow–Teller transition.The mentioned difference is due to configuration mixing and the ground state correlations considered by us.

To evaluate the $T_{1/2}^{\beta^+}$ value remember the formula for Gamow–Teller transitions [31]:

$$T_{1/2}(GT) \;=\; \frac{6163}{(g_A/g_V)^2 f_0(Q_\beta, Z) B(GT)} \;. \tag{33}$$

Here f_0 is an integral Fermi function for allowed beta-transition

$$f_0(Q_\beta, Z) \;=\; F_0(E_\beta \equiv Q_\beta/m_e c^2 + 1) \cdot S(Q_\beta, Z) \;, \tag{34}$$

where

$$F_0(E_\beta) \;=\; \frac{1}{60}(E_\beta^2 - 1)^{1/2}(2E_\beta^4 - 9E_\beta^2 - 8) + \frac{1}{4}\, E_\beta \ln\left(E_\beta + \sqrt{E_\beta^2 - 1}\right) \tag{35}$$

– is a Fermi function for zero charge, while $S(Q_\beta, Z)$ is a screening function.

Taking for the purpose of evaluation the magnitude of $|g_A/g_V|$ in nuclear media equal to 1 and $S(Q_{\beta^+} = 9.02 \text{ MeV}, Z = 82) \approx 0.32$ [32], we obtain $T_{1/2}(\beta^+) = 13$ ms.

As one can see from Fig. 3 the difference of binding energies of related isobaric states in ^{164}Pb and ^{164}Tl (for example, 10^+ states), presenting the difference of Coulomb energies of the mentioned nuclei, occurs to be about 19 MeV. In the model of uniformly charged sphere having the radius $R_c = r_{oc} \cdot A^{1/3}$ the Coulomb energy of the (A, Z) nucleus and the difference of Coulomb energies of the (A, Z) and $(A, Z-1)$ nuclei are correspondingly equal to

$$E_{\mathrm{Coulomb}} = \frac{3}{5}\,\frac{e^2}{r_{oc}}\,\frac{Z(Z-1)}{A^{1/3}} \;, \quad \Delta E_{\mathrm{Coulomb}} = 0.864 \frac{(2Z-2)}{r_{oc}(\mathrm{fm}) \cdot A^{1/3}} \text{ MeV} \;, \tag{36}$$

from which we obtain $r_{oc} = 1.34$ fm. This number is about $8 - 10\%$ more than the analogous value usually obtained from the electron scattering and used by us in phenomenological potential (2). The difference is due to exchange Coulomb interaction that decreases the Coulomb

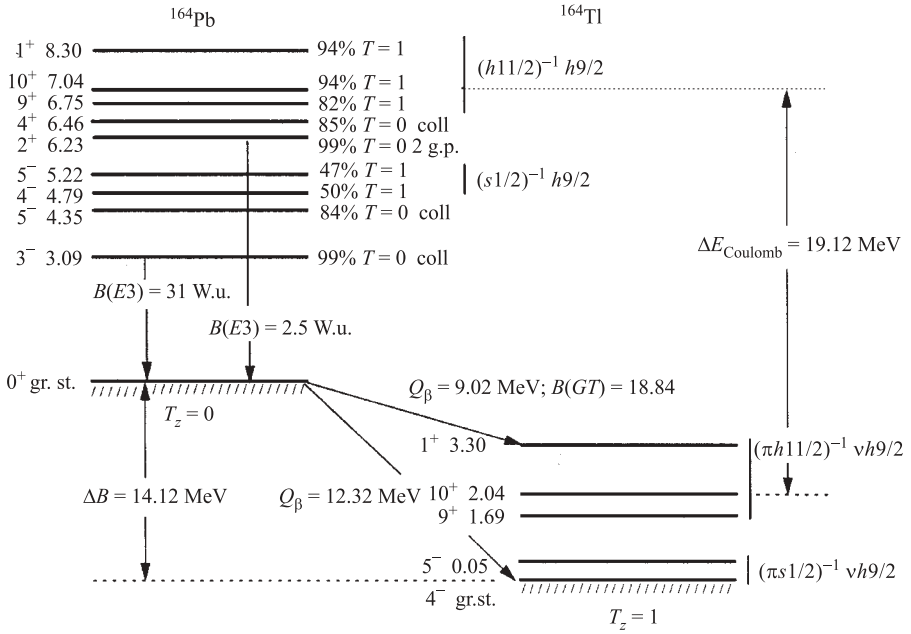

Fig. 3. Properties of isobaric nuclei with $A = 164$

energy. Such interaction was included in our self consistent calculation, but ignored by the formulas (36). We note here that if we use the single-particle spectrum of phenomenological potential (variant $Stnd$ of Tables 6 and 7), the difference of Coulomb energies corresponds to $r_{oc} = 1.23$ fm, which practically coincides with the value of this parameter in the initial potential.

Turning again to the excitation spectra of ^{164}Pb we note that the lowest excited states here are the collective isoscalar 3^- and 5^- levels.The collectivity of 3^- state (30 W.u.) is slightly less than in ^{208}Pb (experimental value 34 W.u.) and exceed that in ^{132}Sn (the indirect estimate ~ 15 W.u. from the experimental [33] value of octupole effective charge in ^{134}Te and > 10 W.u. from the experimental limit on the half-life of the 3^-_1 level in ^{132}Sn [2]). At the same time, the lowest isoscalar 2^+ and 4^+ states lie much higher. The collectivity of 4^+ is rather strong (~ 14 W.u.), while that for the 2^+-state is small ($\sim 2-3$ W.u.) being also strongly dependent on the relative position of the proton 1h9/2 and 2f7/2 states. The last quantity should be compared with the $B(E2; 2^+_1 \to$ gr. st.) value in ^{208}Pb (~ 8 W.u.) and with the indirect estimate [34] of this characteristic in ^{132}Sn, obtained from the value of an effective quadrupole charge in nuclei close to ^{132}Sn and equal to $8-10$ W.u. We note here that as the diagrams that define the structure of phonon are similar to those contributing the magnitude of the effective charge, the $B(E\lambda)$ values presented above were obtained by using the «bare» (e_p = 1 and e_n = 0) values of effective charges. However the basis used in our RPA calculations (one shell above and the other one, with the opposite parity, – below the Fermi level for each sort of nucleons) may be not enough for saturating the values of effective charges of the positive parity $E2$ transitions. This leads to the necessity of introducing the e_p and e_n values corresponding to nuclear media. In case of γ-decay of the isoscalar 2^+_1

Table 6. Single-particle proton energies of the ^{164}Pb nuclide, corresponding to different phenomenological potentials

$n\ell j$	$Set3$	$Stnd$	BEn
$3p1/2$	11.39(670)	10.68(570)	10.37(446)
$3p3/2$	10.22(302)	9.75(284)	9.33(190)
$2f5/2$	10.71(74)	10.43(88)	10.17(66)
$1i13/2$	7.58(7.08 E-3)	9.30(1.99 E-1)	8.42(4.86 E-2)
$2f7/2$	7.59(1.92)	7.80(4.02)	7.21(1.42)
$1h9/2$	6.72(3.22 E-3)	7.89(5.74 E-2)	7.65(3.44 E-2)
$3s1/2$	3.27(1.28 E-5)	3.37(3.62 E-5)	2.87(1.02 E-6)
$2d3/2$	2.76(4.04 E-8)	3.06(6.76 E-7)	2.65(2.22 E-8)
$1h11/2$	0.81(1.20 E-28)	2.49(1.39 E-11)	1.66(1.57 E-16)
$2d5/2$	0.68(2.18 E-29)	1.22(2.14 E-18)	0.59(2.22 E-32)
$1g7/2$	-1.40	-0.08	-0.44

The values of energies are given in MeV, while the widths of unbound states (in brackets) – in keV. Potential $Set3$ uses the parameters, defined by us in [24] for ^{100}Sn, potential $Stnd$ is borrowed from our works [19], [20], [23], while the BEn set reproduces the separation energies of protons and neutrons in isotopes from ^{132}Sn to ^{100}Sn.

Table 7. Single-particle neutron energies of ^{164}Pb, corresponding to phenomenological Woods-Saxon potentials

$n\ell j$	$Set3$	$Stnd$	BEn
$3p1/2$	-8.34	-8.49	-7.70
$3p3/2$	-9.58	-9.62	-8.92
$2f5/2$	-9.28	-9.55	-8.63
$1i13/2$	-10.94	-10.79	-10.29
$2f7/2$	-12.40	-12.39	-11.72
$1h9/2$	-12.93	-13.37	-12.31
$3s1/2$	-17.81	-17.95	-17.11
$2d3/2$	-18.17	-18.41	-17.48
$1h11/2$	-18.27	-18.21	-17.59
$2d5/2$	-20.13	-20.20	-19.42
$1g7/2$	-21.55	-21.91	-20.88

Potential $Set3$ uses the parameters, defined in [24] for nuclide ^{100}Sn, potential $Stnd$ corresponds to works [19], [20], [23], while the BEn variant gives the best description of the proton and neutron separation energies in the chain of isotopes from ^{132}Sn to ^{100}Sn.

state in ^{164}Pb, having the symmetric spin-coordinate function, this leads to increase of the $B(E2)$ value presented above in $(e_p + e_n)^2 \approx 2.5^2$ times, where we used the experimental magnitudes of quadrupole effective charges for nuclei close to ^{208}Pb. The resulting value of about 17 W.u. presents the maximal estimate of the $E2$ transition probability of the lowest 2^+ state in ^{164}Pb, corresponding to coherent contribution of proton and neutron non-spin-flip 1h11/2 $\rightarrow$ 2f7/2 single-particle $E2$ transition matrix elements.

4.3. Proton Radioactivity. As the ^{164}Pb nucleus is an extremely neutron deficient one and evidently lies outside the border of proton stability (see Tables 2 and 3), it's most probable decay mode is expected to be the emission of a proton. Therefore we examine in this section the problem of the widths of proton unbound states in this nuclide. These widths were calculated by us in the framework of the integral method, elaborated in [26, 27].

If the mean field potential that forms the «pocket» responsible for appearing of the quasi-stationary state is composed of two items, namely the attraction (for example, the nuclear

part of the mean field potential (2)) and the repulsion (Coulomb and the centrifugal parts of potential), then the formula for the width of a quasi-stationary state looks as:

$$\Gamma_{n\ell j} \;=\; 2\pi \left| \int\limits_0^{\sim r_>} R_{n\ell j}(r) U_{\rm nucl}(r) \phi^{\varepsilon}_{\ell}(r) dr \right|^2 \cdot S_{n\ell j} \; . \tag{37}$$

Here $R_{n\ell j}$ is a radial eigenfunction of a quasi-stationary level, normalized to unity in the interval from zero up to the external turning point $r_>$, and corresponding to the sum of nuclear $U_{\rm nucl}$, Coulomb U_c and centrifugal $U_{\ell\ell}$ potentials (shell model radial function). Those are the functions defined by us earlier by the finding of the real parts of the (positive) mean field eigenvalues, $\varepsilon_{n\ell j}$, and used in particular in our shell model and self consistent calculations. The function $\phi^{\varepsilon}_{\ell}(r)$, entering formula (37), presents the regular Coulomb function of continuum, corresponding to the energy ε and orbital moment ℓ, defined with the account of the finite size of a nucleus and normalized to δ- function in energy. By $r \to \infty$ it has the asymptotics

$$\phi^{\varepsilon}_{\ell}(r \to \infty) \;\longrightarrow\; \frac{1}{\hbar}\sqrt{\frac{2m}{\pi k}} \sin\left(kr - \frac{\ell\pi}{2} - \eta \ln(2kr) + \sigma_\ell + \delta_\ell \right), \tag{38}$$

where $k = (\sqrt{2m\varepsilon})/\hbar$, $\eta = (mZe^2)/(\hbar^2 k)$, $\sigma_\ell = \arg\Gamma(i\eta + \ell + 1)$ is a Coulomb phase, while δ_ℓ is an additional small phase shift considering the finite size of a charge distribution in nucleus. The functions ϕ were found by numerical integration from $r = 0$ with the corresponding boundary condition. The normalization of these functions as well as the phase shift δ_ℓ (small for sub-barrier energies) were defined by matching the numerical solution at $r > R_c$ with the sum of properly normalized (see for example (38)) regular F_ℓ and irregular G_ℓ Coulomb functions for the point-like distribution of nuclear charge.

The quantity $S_{n\ell j}$ in (37) presents the spectroscopical factor of single-particle state, corresponding to it's spread over the states of more complicated nature. As we consider here nuclei close to the doubly magic one, the values of $S_{n\ell j}$ are supposed to be equal to unity, which corresponds to the well-known experimental situation, for example for ^{208}Pb, where $S \sim 0.7 - 0.9$.

The results of calculation of proton widths Γ^p obtained by using the formula (37) are presented in Table 6. Qualitatively close values of Γ^p were obtained by using the formula analogous to (31) for protons, if one takes the values $\Gamma_0 \sim \hbar\omega_{\rm osc}/2\pi$ with $\hbar\omega_{\rm osc} = 41/A^{1/3}$ MeV and the functions $U^p_{\rm opt}(r)$, that coincide with the corresponding nuclear potentials for protons.

Turning to the evaluation of $T^p_{1/2}$ for the proton decay of ^{164}Pb we note that, as it follows from the single-particle schemes presented in Tables 4 and 6, it is defined by the width of the decay to the $3s_{1/2}$ state of ^{163}Tl. The energy of this decay, as one can see from our calculations (see Table 1) is weakly dependent on the variant of the mean field and offers a value of about 3 MeV. The width of the mentioned level, that has no centrifugal barrier, is defined only by the Coulomb field and presents the value of about $0.001 \div 0.04$ electron–volts, which corresponds to the lifetime of about $1 \div 0.025$ ps. It is just the decay that defines the degree of (un)stability of ^{164}Pb, because the two- proton decay, which is also possible here, is substantially weaker than the one-proton transition.

4.4. Spontaneous Fission. The receiving of a reliable evaluation for the half-life of ^{164}Pb relatively to the spontaneous fission presents a complicated problem that includes the determination of the form and the height of fission barrier, calculation of the reduced width and finding of corresponding dynamical mass parameters that influence the process of fission. Here we simplificate the problem limiting by some available and rather simple ideas.

We mention first that the values of the fissility parameter «x» (see [35]),

$$x = \frac{Z^2/A}{51.77 \cdot [1 - 1.79\,(\frac{N-Z}{A})^2]} \tag{39}$$

for nuclei ^{208}Pb, ^{238}U, and ^{164}Pb are equal to 0.678, 0.757, and 0.792 correspondingly. Thus we see that as compared to ^{238}U the fissility of ^{164}Pb increases not too much which is mainly due to the absence of the symmetry term in the surface energy of this nucleus. Note that $T^f_{1/2}$ for the ^{238}U is a value of the order of 10^{16} y., this value being much more for ^{208}Pb (the decay is not seen in the experiment). In [36] in the framework of the macroscopic–microscopic model accounting for shell corrections [35] different global characteristics of nuclei, including the fission barriers, were defined. The minimal value of N at $Z = 82$, for which the barrier was calculated in [36] is $N = 84$. Short extrapolation of the results [37] to $Z = N = 82$ gives the value of $B_f \approx 11.2$ MeV. Using the results of [37] we have the following formulas for definition of the spontaneous decay width, obtained in the approach that potential between fragments has the form of two matched, «convex-up» and «convex-down», parabolas:

$$\Gamma_f = \frac{\hbar\omega_{gs}}{2\pi} \exp\left[-\frac{2\pi(B_f - \frac{1}{2}\hbar\omega_{gs})}{|\hbar\omega_2|}\right], \tag{40}$$

where

$$\hbar\omega_{gs} = \hbar\left[\frac{8}{3}(1-x)\right]^{1/2} \cdot \left[\frac{E^0_s}{M_0 R_0^2}\right]^{1/2} \tag{41}$$

with

$$\hbar\left[\frac{E^0_s}{M_0 R_0^2}\right]^{1/2} = 23.12 \cdot \frac{[1 - 1.79\,(\frac{N-Z}{A})^2]^{1/2}}{A^{1/2}}\,\text{MeV}. \tag{42}$$

For ^{164}Pb, as follows from Fig. 8 of [37], we obtain

$$|\hbar\omega_2| \approx 0.48 \cdot \left[\frac{E^0_s}{M_0 R_0^2}\right]^{1/2} \hbar. \tag{43}$$

As a result, we have for the asymmetric fission of ^{164}Pb the value of $T^f_{1/2} \sim 10^5$ years.

One may offer another estimate based on the relation of the type (32) but for fission, with normalization to the spontaneous fission of ^{238}U (for certainty we considered the decay ^{238}U $\rightarrow$ ^{132}Sn + ^{106}Mo with $Q_f \approx 200$ MeV). Considering the decay ^{164}Pb $\rightarrow$ ^{100}Sn + ^{64}Ge with $Q_f \sim 170$ MeV, assuming the equality of the reduced widths in both cases (which is much less evident than for the α decay studied by us before) and assuming also that the corresponding nuclear potentials between the fragments have the rectangle-well shape with $R_{12} = 1.25(A_1^{1/3} + A_2^{1/3})$ fm, we obtain the value $T^f_{1/2} \sim 10^{12}$ y. We note here that the difference between the two estimates in seven orders of magnitude, as can be seen from formulas (40) and (43), corresponds to the increase of the B_f magnitude used by us by the value of one MeV, what is not too excessive.

5. DISCUSSION AND CONCLUSION

As was already mentioned, the calculations undertaken in this work within the framework of the shell model approach are valid if the $Z = N = 82$ nucleon numbers are assumed as magic ones. However this prerequisite can be considered rather as possible than obligatory. The «universality» of magic numbers is still an open question. Indeed, recently [13] the analysis of behavior of the two- proton separation energies S_{2p} showed the washing out of gap in the S_{2p}-values towards the proton drip-line (when the neutron numbers become less than ≈ 114). As it was noted in [13] this behavior is a particular property of the $Z = 82$ region and reflects the changes in the nuclear structure for single-magic neutron-deficient nuclides in the lead region. Nevertheless we can expect that due to the effect of «mutual support of magicities» [38], which works in doubly magic nuclides, the closed shell structure can be restored for the $Z = N = 82$ nuclide. In this case the results of the shell model calculations performed in this work can be considered as quite trustworthy. In addition, it is worthy to emphasize here that the same magic spectroscopic characteristics for ^{164}Pb have been obtained as well by different, self-consistent approach (see Section 3), though one can see numerical difference for some Q-values calculated in the framework of two methods.

As can be seen from the results of previous section and Tables 2 and 3, the most probable decay in the close vicinity to ^{164}Pb is a proton disintegration of nuclide. The partial proton-decay half-life is expected not to be exceedingly small for the lead-164 nuclide and can, in principle, be measured directly. The new generation Radioactive Ion Beam facilities could be used for production of the lead isotopes in the region though very small half-lives and cross-sections in spallation-fragmentation or fusion-evaporation reactions will lead to difficulty in their observation.

At the same time one should mention that our estimate of the half-life of ^{164}Pb relatively to the proton decay is strongly based on the structure of the proton single-particle spectrum near the Fermi surface of this nuclide. One should hope that the Nature may be more kind to us and so the problem of discovering this nuclide may really become more realistic. This is especially true if one shall try to identify this nuclide by detecting all the cascade of decays that lead to the final daughter nucleus which is more stable and which can be reliably identified.

This work was supported by the Russian Foundation for Basic Research (grant No. 96-15-96764 in support of the Leading Science Schools). The authors are grateful to Prof. J. Blomqvist for valuable discussion.

References

1. Isakov V.I., Mezilev K.A., Novikov Yu.N. et al. — Preprint PNPI-2309, 1999; Physics of Atomic Nuclei, 2000, v. 63, No. 10.

2. Fogelberg B., Hellstrom M., Jerrestam D. et al. — Phys. Scripta, 1995, v.T56, p.79.

3. Mezilev K.A., Novikov Yu.N., Popov A.V., Fogelberg B., Spanier L. — Phys. Scripta, 1995, v.T56, p.272.

4. Blomqvist J. — 4th Int. Conf. on Nuclei Far from Stability. Helsingor; CERN Report 81-09, 1981, p.536.

5. Schneider R., Friese J., Reinhold J. et al. — Z. Phys., 1994, v.A348, p.241.
6. Lewitowicz M., Anne R., Auger G. et al. — Phys. Lett., 1994, v.B332, p.20.
7. Grawe H., Shubart R., Maier K.H., Seweryniak D. — Physica Scripta, 1995, v.T56, p.71.
8. Chartier M., Auger G., Mittig W. et al. — Phys. Rev. Lett., 1996, v.77, p.2400.
9. Grawe H., Gorska M. et al. — Progr. Nucl. Phys., 1997, v.38, p.15.
10. Lipoglavsek M., Seweryniak D., Davids C.N. et al. — Phys. Lett., 1998, v.B440, p.246.
11. Zeldes N. — Ark. Fyz., 1967, v.36, p.361.
12. Nazarewicz W., Dobaczewski J. et al. — Phys. Rev., 1996, v.C53, p.740.
13. Novikov Yu.N., Radon T. et al. — Nucl. Phys. A (to be submitted).
14. Shalit A., Talmi I. — Nuclear Shell Theory. New York–London, Acad. Press, 1963.
15. Vautherin D., Brink D.M. — Phys. Rev., 1972, v.C5, p.626.
16. Soloviev V.G. — Theory of Complex Nuclei. Moscow: Nauka, 1971.
17. Beiner M., Flocard H., Nguen Van Giai, Quentin P. — Nucl. Phys., 1975, v.A238, p.29.
18. Waroquier M., Sau J., Heyde K., Van Isacker P., Vinex H. — Phys. Rev., 1973, v.C19, p.1983.
19. Erokhina K.I., Isakov V.I. — Izv. RAN, ser. fiz., 1992, v.56, p.78.
20. Erokhina K.I., Isakov V.I. — Physics of Atomic Nuclei, 1994, v.57, p.198.
21. Isakov V.I., Artamonov S.A., Sliv L.A. — Izv. AN SSSR, ser. fiz., 1977, v.41, p.2074.
22. Mach H., Jerrestam D., Fogelberg B. et al. — Phys. Rev., 1995, v.C51, p.500.
23. Erokhina K.I., Isakov V.I. — Physics of Atomic Nuclei, 1996, v.59, p.589.
24. Isakov V.I., Erokhina K.I., Mach H., Sanchez-Vega M., Fogelberg B. — Preprint PNPI-2308, 1999.
25. Artamonov S.A., Isakov V.I., Kadmensky S.G., Lomachenkov I.A., Furman V.I. — Sov. J. Nucl. Phys., 1982, v.36, p.486.
26. Kadmensky S.G., Kalechits V.E. — Sov. J. Nucl. Phys., 1971, v.12, p.37.
27. Kadmensky S.G., Furman V.I. — Sov. J. Part. Nucl., 1975, v.6, p.189.
28. Igo G. — Phys. Rev. Lett., 1958, v.1, p.72.
29. Rasmussen J.O. — Phys. Rev., 1959, v.113, p.1563.
30. Barnett A.R., Lille J.S. — Phys. Rev., 1974, v.C9, p.2010.

31. Bohr A., Mottelson B.R. — Nuclear Structure, vol.1, Benjamin Press, New York–Amsterdam, 1969.

32. Dzelepov B.S., Zyrianova L.N., Suslov Yu.P. — Beta-Processes. Leningrad: Nauka,1972.

33. Omtvedt J.P., Mach H., Fogelberg B. et al. — Phys. Rev. Lett., 1995, v.75, p.3090.

34. Erokhina K.I., Isakov V.I., Fogelberg B., Mach H. — Preprint PNPI-2225, 1998.

35. Myers W.D., Swiatecki W.J. — Nucl. Phys., 1966, v.81, p.1.

36. Myers W.D., Swiatecki W.J. — UCRL Report-11980, 1967.

37. Nix J.R. — Annals of Physics, 1967, v.41, p.52.

38. Schmidt K.-H., Vermeulen D. — Proc. AMCO-6 Conference, ed. by J. Nolen and W. Benenson, New York–London, 1979, p.119.

Received on November 11, 2000.